Peer-reviewed version available at *Viruses* **2019**, *11*, 354; doi:10.3390/v11040354

Article

First description of a natural infection with Shrimp hemocyte iridescent virus in farmed giant freshwater prawn, *Macrobrachium rosenbergii*

Liang Qiu [1,#], Xing Chen [1,2,#], Ruo-Heng Zhao [1,3], Chen Li [1], Wen Gao [1,2] Qing-Li Zhang [1,2], and Jie Huang [1,2,3,*]

[1] Yellow Sea Fisheries Research Institute, Chinese Academy of Fishery Sciences; Laboratory for Marine Fisheries Science and Food Production Processes, National Laboratory for Marine Science and Technology (Qingdao); Key Laboratory of Maricultural Organism Disease Control, Ministry of Agriculture and Rural Affairs; Qingdao Key Laboratory of Mariculture Epidemiology and Biosecurity; Qingdao 266071, China
[2] Shanghai Ocean University, Shanghai 201306, China
[3] Dalian Ocean University, Dalian 116023, China
[#] These authors contributed to the work equally and should be regarded as co-first authors.
[*] Correspondence: huangjie@ysfri.ac.cn; Tel.: +86-138-0542-1513

Abstract: *Macrobrachium rosenbergii* is a valuable freshwater prawn in Asian aquaculture. In recent years, a new symptom that was generally called as 'white head' caused high mortality in *M. rosenbergii* farms in China. Samples of *M. rosenbergii*, *M. nipponense*, *Procambarus clarkii*, *M. superbum*, *Penaeus vannamei*, and Cladocera from a farm suffering from 'white head' in Jiangsu Province were collected and analyzed in this study. Pathogen detection showed that all samples were positive for Shrimp hemocyte iridescent virus (SHIV). Histopathological examination revealed dark eosinophilic inclusions and pyknosis in hematopoietic tissue, hepatopancreas and gills of *M. rosenbergii* and *M. nipponense*. Blue signals of *in situ* DIG-labeled LAMP (ISDL) appeared in hematopoietic tissue, hemocytes, hepatopancreatic sinus, and antennal gland. TEM of ultrathin sections showed a large number of SHIV particles with a mean diameter about 157.9 nm. The virogenic stromata and budding virions were observed in hematopoietic cells. Quantitative detection by TaqMan probe based real-time PCR of different tissues in natural infected *M. rosenbergii* showed that hematopoietic tissue contained the highest SHIV load with a relative abundance of (25.4±16.9)%. Hepatopancreas and muscle contained the lowest SHIV load with a relative abundance at (2.44±1.24)% and (2.44±2.16)%, respectively. Above results verified that SHIV is the pathogen causing 'white head' in *M. rosenbergii*, and *M. nipponense* and *Pr. clarkii* are also the susceptible species of SHIV.

Keywords: SHIV; *Macrobrachium rosenbergii*; *Macrobrachium nipponense*; *Procambarus clarkii*; white head; Histopathology; Susceptible species; Viral load

1. Introduction

Globally, viral diseases have been acknowledged as a huge threat to shrimp aquaculture industry. Among the viruses reported for crustacean, Shrimp hemocyte iridescent virus (SHIV) was a newly found virus isolated from diseased white leg shrimp *Penaeus vannamei* in December of 2014 in Zhejiang Province of China, which can cause massive mortality to *P. vannamei* [1], the most important crustacean for global aquaculture. The virus has a typical icosahedral structure with a mean diameter around 150 nm [1]. Evidences from histopathological study, transmission electron microscope (TEM) of ultrathin sections, and *in situ* hybridization (ISH) indicated that SHIV may mainly infect the hematopoietic tissue and hemocytes in *P. vannamei* [1]. SHIV has a double-stranded DNA genome of 165,809 bp. Phylogenetic analysis supported that SHIV belong to a new genus,

which was originally proposed to name as *Xiairidovirus*, in family *Iridoviridae* [2]. Alignment of the complete genome sequences revealed that SHIV and *Cherax quadricarinatus* iridovirus (CQIV), a new iridescent virus identified from freshwater red claw crayfish *Cherax quadricarinatus*, might be the different strains or genotypes of the same virus species [2-5]. SHIV has been detected in farmed penaeid shrimp *P. vannamei*, *P. chinensis*, and giant freshwater prawn *Macrobrachium rosenbergii* in some coastal provinces of China since 2014 [1] and also been reported in Thailand recently [6], indicating that SHIV is a new threat to the shrimp farming industry.

The giant freshwater prawn, *M. rosenbergii*, is a valuable crustacean species in Asian aquaculture, being widely cultured in tropical and subtropical areas. *M. rosenbergii* is native to Malaysia and other Asian countries, including Vietnam, Cambodia, Thailand, Myanmar, Bangladesh, India, Sri Lanka, and the Philippines [7,8]. Being popular for its delicious flesh and high nutritive value, the global production of this species has increased from about 3,000 tons in 1980 to more than 220,000 tons in 2014 [9,10]. Generally, *M. rosenbergii* is considered less prone to some viral diseases in culture when compared to penaeid shrimps [11]. Some viral pathogens such as *Macrobrachium* hepatopancreatic parvo-like virus (MHPV), *Macrobrachium* muscle virus (MMV), Infectious hypodermal and hematopoietic necrosis virus (IHHNV), White spot syndrome virus (WSSV), *Macrobrachium rosenbergii* nodavirus (MrNV), and Extra small virus like particle (XSV) have been reported in the prawn [12]. Recently, results of RT-LAMP and histopathological examination indicated that *M. rosenbergii* could be infected with Covert mortality nodavirus (CMNV) [13]. To date, only PCR results showed that cultured *M. rosenbergii* were SHIV positive [1, 14] and more pathological information are not available.

In recent years, a new symptom that occurred in the *M. rosenbergii* farms in China was commonly called as 'white head' or 'white spot' due to the diseased prawn exhibited a significant white triangle under the carapace at the base of rostrum [15]. Moribund prawns hiding on the bottom in deep water and dead prawns could be found every day with a cumulative mortality up to 80%. It is noteworthy that many *M. rosenbergii* populations suffering from 'white head' were polycultured with *P. vannamei* [16]. In the present study, we investigated a diseased polyculture pond with *M. rosenbergii* and *Pr. clarkii*. In the pond, most of *M. rosenbergii* exhibited typical white triangle under the carapace at the base of rostrum and appeared moribund or died. One-month before we arrived, all of *P. vannamei* in an adjacent pond have died. Samples were collected and analyzed in this study.

2. Materials and Methods

All the protocols of animal handling and sampling were approved by the Animal Care and Ethics Committee, Yellow Sea Fisheries Research Institute, Chinese Academy of Fishery Sciences, and all efforts were made to minimize the suffering of animals according to recommendations proposed by the European Commission (1997). The study was carried out in accordance with the approved protocol. All the methods were applied in accordance with relevant guidelines.

2.1 Samples

Samples of farmed *M. rosenbergii* (4-6 cm) and *Pr. clarkii* (5-7 cm) were collected from the pond with high mortality in a farm in Jiangsu Province on 20 June 2018. In the same pond, some wild crustaceans, including *M. nipponense*, *M. superbum*, and some species of Cladocera, also been sampled for further analysis. Died and dry bodies of *P. vannamei* (5-7 cm) were collected on the drained bottom of the adjacent pond suffered from a severe disease one month before in the farm.

2.2 DNA and RNA extraction

Total DNA and RNA was extracted from 30 mg cephalothorax tissue of prawns, shrimp, or crayfish or 30 mg multiple individuals of Cladocera by TIANamp Marine Animal DNA Kit and RNAprep pure Tissue Kit (TIANGEN Biotech, Beijing, China), respectively, according to the manufacturer's instructions.

2.3 Pathogen detection

The DNA samples of *M. rosenbergii*, *P. vannamei*, *Pr. clarkii*, *M. nipponense*, *M. superbum*, and Cladocera were tested for White spot syndrome virus (WSSV), IHHNV, acute hepatopancreas necrosis disease-causing *Vibrio parahaemolyticus* (*Vp*$_{AHPND}$), and SHIV by real-time PCR methods. The RNA samples were tested for Yellow head virus (YHV), Infectious myonecrosis virus (IMNV), and CMNV by RT-real-time PCR methods. All the detection methods are recommended by the World Organization for Animal Health [17] or developed before [3,18].

2.4 Histopathological sections

Samples were fixed in Davidson's alcohol-formalin-acetic acid fixative (DAFA) [19] for 24 h and then changed to 70% ethanol. Paraffin sections were prepared and stained with hematoxylin and eosin (H&E) staining according to the procedures of Bell & Lightner [19].

2.5 In situ DIG-labeling, *loop-mediated isothermal amplification (ISDL)*

Samples were fixed in DAFA for 24 h and changed to 70% ethanol. The paraffin sections were then prepared and subjected to ISDL assays targeting the gene of DNA-directed RNA polymerase II second largest subunit for SHIV according to the method adapted for SHIV infection by Chen et al. [20].

2.6 Transmission electron microscopy (TEM)

Ultrathin sections of the white triangle tissue under cuticle at the base of rostrum (hematopoietic tissue) from diseased *M. rosenbergii* were prepared for observation with TEM. Small pieces of the hematopoietic tissue in about 1 mm^3 of sampled animals were fixed in TEM fixative (2% paraformaldehyde, 2.5% glutaraldehyde, 160 mM NaCl, and 4 mM $CaCl_2$ in 200 mM PBS) (pH 7.2) for 24 h at 4 °C. Before ultrathin sectioning, the fixed tissues were secondarily fixed with 1% osmium tetroxide for 2 h, then embedded in Spurr's resin and stained with uranyl acetate and lead citrate. Ultrathin sections were laid on collodion-coated grids and examined under a JEOL JEM-1200 electron microscope (Jeol Solutions for Innovation, Japan) operating at 80–100 kV in the Equipment Center of the Medical College of Qingdao University.

2.7 Quantitative detection of SHIV in different tissues of natural infected M. rosenbergii

Total 15 moribund *M. rosenbergii* samples frozen at -80 °C were chosen to defrost and separate different tissues, including hematopoietic tissue, antenna, uropods, pleopods, gills, pereiopods, muscle and hepatopancreas. Total DNA was extracted from different tissues using TIANamp Marine Animal DNA Kit. The SHIV loads in different tissues were detected by TaqMan probe based quantitative real-time PCR (TaqMan qPCR) following our previous published method [3].

2.8 Relative abundance of SHIV in different tissues

In order to evaluate the distribution of SHIV in different tissues, the relative abundance (RA_i) of SHIV in different tissues was calculated with the SHIV load in each tissue (L_i) to compare with the total load of SHIV in the whole body, which were resulted from the sum of the SHIV loads in all tested tissues ($\sum L_i$). The calculation based on the following formula:

$$RA_i = \frac{L_i}{\sum L_i}$$

Significance analysis of relative abundance data between each two tissues was carried out using the t-test for heteroscedasticity hypothesis of two group of samples with the add-in tool of Data Analysis in Microsoft® Excel® 2016 MSO 64-bit.

3. Results

3.1 Observation of clinical signs of diseaesd M. rosenbergii

According to on-farm inquiry, the investigated pond about 1.5 ha in size was stocked with 45 postlarva/m^2 of prawn *M. rosenbergii* in the middle of May and some juveniles of crayfish *Pr. clarkii* one week before. The adjacent pond stocked with shrimp *P. vannamei* suffered from an unknown disease and died out one month before. No disinfection or other effective control measure was taken for the ponds except of the diseased shrimp pond. Symptoms of 'white head' and 'yellow gills' in the prawn population were observed two weeks before our arrival. During the first week, the disease developed slowly, but it became more and more severe in the second week. The moribund prawns lost their swimming ability and sank to the bottom of water and were rarely found in shallow water. Moribund and dead prawns could be found every day in diseased pond. In the following inquiry, we were told that the cumulative mortality was more than 80%.

While the samples were taken and processed, it was observed that most caught prawns *M. rosenbergii* from the diseased pond exhibited obvious clinical signs, including a distinct white triangle area under the carapace at the base of rostrum, hepatopancreatic atrophy with colour fading and yellowing in the section, empty stomach and guts (Figure 1, A and B), and some moribund prawns were accompanied by slightly whitish muscle and mutilated antenna.

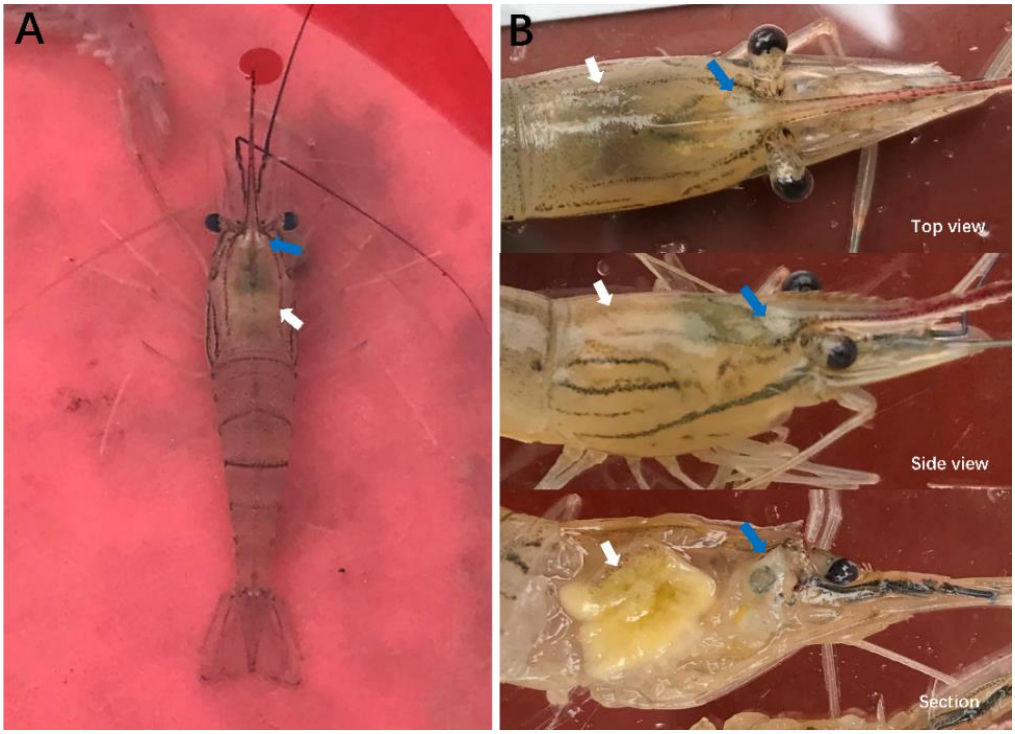

Figure 1. Clinical symptoms of *M. rosenbergii* (20180620) natural infected with SHIV. **A:** Overall appearance of a diseased prawn in water; **B:** Close-up of cephalothoraxes. Blue arrows show white area under the cuticle at the base of rostrum. White arrows indicate hepatopancreas atrophy, colour fading and yellowing.

3.2 Pathogen detection of samples

A total of 20 DNA samples extracted from cephalothorax tissues or multiple Cladocera were tested by real-time PCR or RT-real-time PCR. All samples were negative for WSSV, IHHNV, *Vp*$_{AHPND}$, YHV, IMNV, CMNV, but positive for SHIV. Samples of *M. rosenbergii* contained the highest SHIV load range from 3.16×10^8 to 9.83×10^8 copies/μg-DNA. Samples of *M. superbum* contained the lowest SHIV load. (Table 1)

Table 1. Samples detected with the real time PCR for SHIV.

Species	Positive samples	Total samples	Geometric mean (copies/μg-DNA)	SHIV range (copies/μg-DNA)
M. rosenbergii	5	5	$10^{(8.65\pm0.21)}$	3.16×10^{8} — 9.83×10^{8}
P. vannamei	3	3	$10^{(5.96\pm0.79)}$	4.56×10^{5} — 7.19×10^{6}
M. nipponense	3	3	$10^{(4.17\pm1.68)}$	1.30×10^{3} — 1.30×10^{6}
Pr. clarkii	5	5	$10^{(3.82\pm0.36)}$	2.20×10^{3} — 1.57×10^{4}
Cladocera	3	3	$10^{(1.10\pm0.06)}$	1.09×10^{1} — 1.43×10^{1}
M. superbum	1	1	$10^{(1.04\pm0.05)}$	1.00×10^{1} — 1.18×10^{1}

3.3 Histopathology

Histological examination of DAFA fixed samples showed that dark eosinophilic inclusions mixed with basophilic tiny staining and karyopyknosis existed in hematopoietic tissue (Figure 2, A) and hemocytes in hepatopancreatic sinus (Figure 2, B), and gills (Figure 2, C) of *M. rosenbergii*. For *M. nipponense* dark eosinophilic inclusions and karyopyknosis were also observed in hepatopancreas (Figure 2, D). No typical histopathological feature was found in the tissue sections of *Pr. Clarkii* and Cladocera.

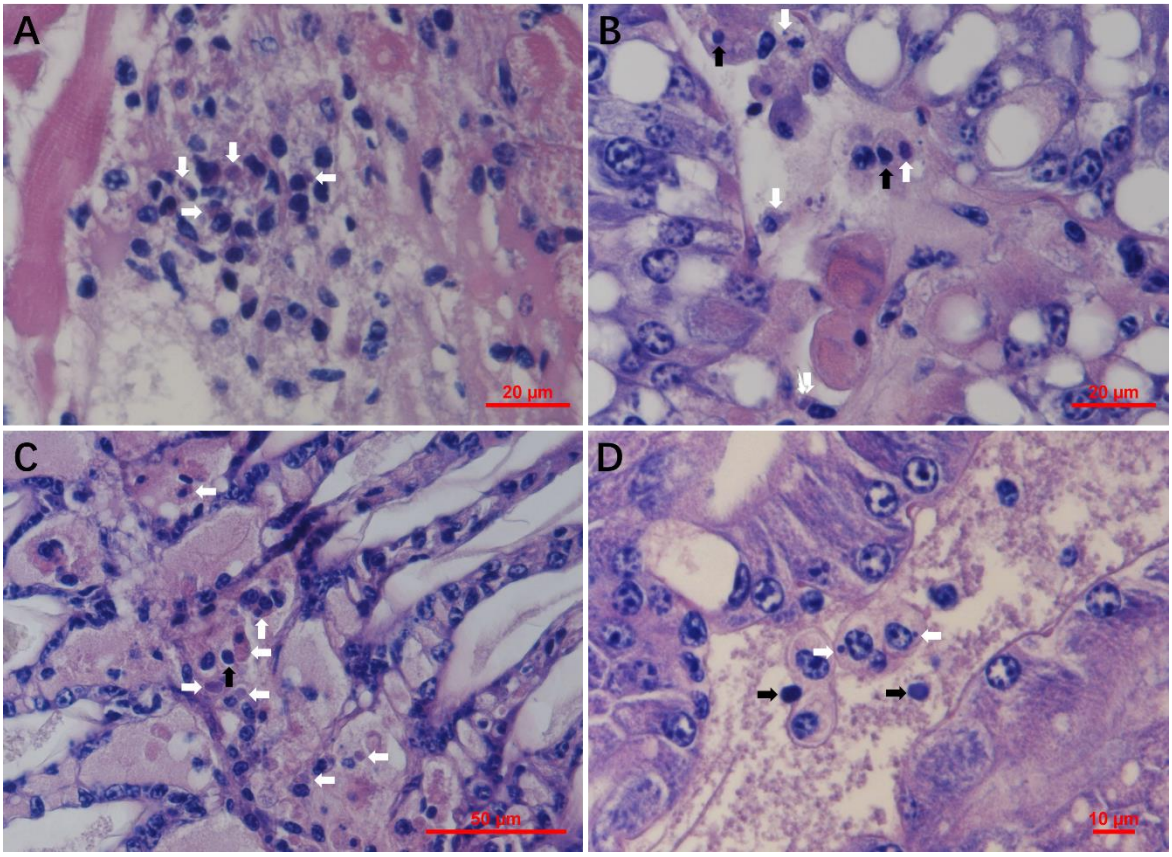

Figure 2. Histopathological features of DAFA fixed *M. rosenbergii* (A, B, and C) and *M. nipponense* (D) samples 20180620. While white arrows show the eosinophilic inclusions and black arrows show the karyopyknotic nuclei. **A**: Hematoxylin and eosin (H&E) staining of the hematopoietic tissue; **B** and **D**: H&E staining of hepatopancreas, and **C**: H&E staining of gills. Bar, 20 μm (A and B), 50 μm (C), and 10 μm (D), respectively.

3.4 ISDL

ISDL results of *M. rosenbergii* showed that blue signals existed in hematopoietic tissue (Figure 3, A) and hemocytes in hepatopancreatic sinus and gills (Figure 3, B and C), some R-cells and myoepithelial fibers of hepatopancreas (Figure 3, D), coelomosac epithelium of antennal gland (Figure 3, E), and epithelium of ovaries (Figure 3, F). In addition, similar distribution of positive

signals was also observed in hepatopancreas of *M. nipponense* (Figure 3G) and hepatopancreas and hematopoietic tissue of *Pr. clarkii* (Figure 3, H and I). No positive signals were observed in sections prepared from Cladocera and uninfected prawn and crayfish.

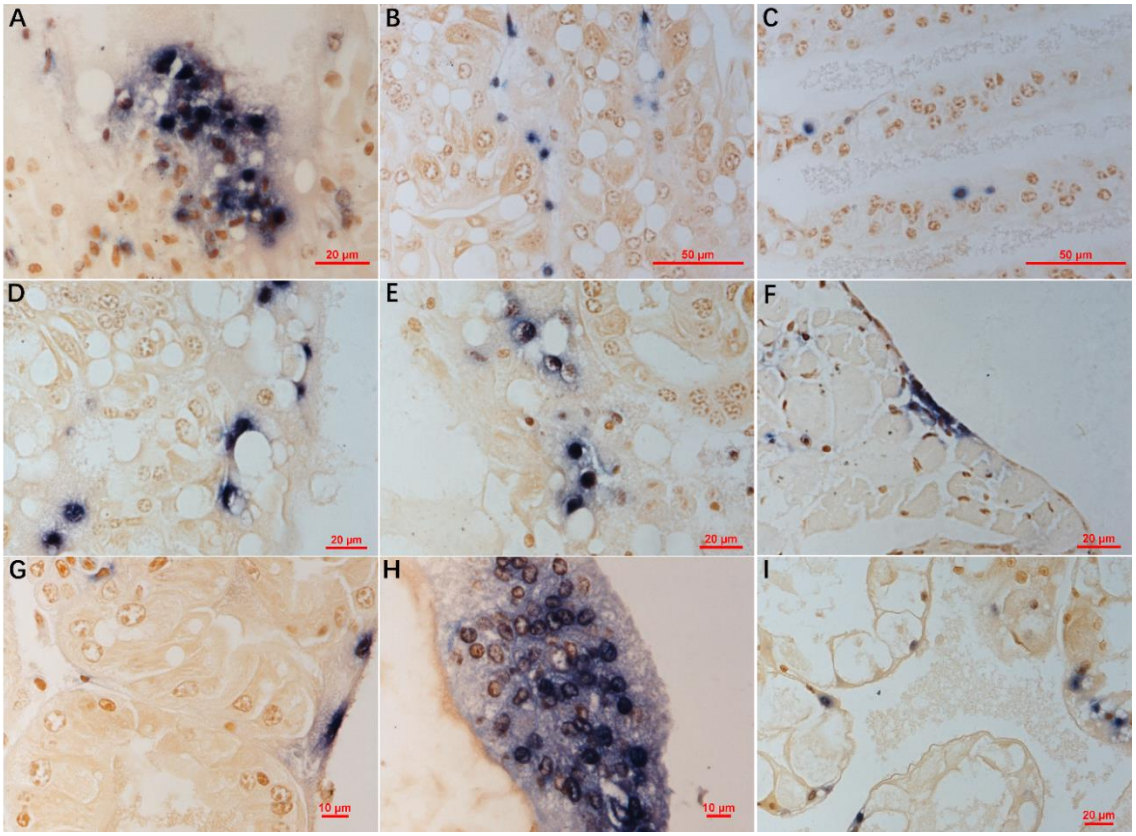

Figure 3. ISDL targeting the DNA-directed RNA polymerase II second largest subunit for SHIV on histological sections of *M. rosenbergii* (A-F), *M. nipponense* (G) and *Pr. clarkii* (H, I) samples 20180620. **A** and **H**: hematopoietic tissue; **B**, **D**, **G**, and **I**: hepatopancreas; **C**: gills; **E**: antennal gland; **F**: ovaries. In A-C, and H, blue signals were observed in hematopoietic tissue, hemocytes in sinus of hepatopancreas and gills. In D, G, and I, blue signals exist in some hepatopancreatic R-cells and myoepithelial fibers. In E, blue signals exist in coelomosac epithelium. In F, blue signals exist in epithelium. Bar, 20 μm (A, D-F, and I), 50 μm (B and C) and 10 μm (G and H), respectively.

3.5 TEM of ultrathin sections

Visualization with TEM of ultrathin sections of the naturally infected *M. rosenbergii* revealed the presence of a large number of icosahedral particles with typical non-enveloped iridescent viral structure both inside and outside hematopoietic cells in hematopoietic tissue (Figure 4, A). Non-enveloped virions were (166.3±14.8) nm (n = 39) vertex to vertex (v-v), (149.4±13.8) nm (n = 39) from face to face (f-f), and about 157.9 nm of an average equivalent diameter, with a nucleoid at (93.5±9.9) nm (n = 39). At the margin of the cytoplasm, there were many virions budding from the plasma membrane (Figure 4, B). Virion formation took place in the cytoplasmic morphologically distinct regions termed virogenic stromata, which were electron-lucent areas containing numerous immature and empty capsids, few mature virions, and devoid of cellular organelles, with paracrystalline array of viral particles and budding virions in the same cell (Figure 4, C and D). During the stage of nucleocapsid formation, crescent-shaped structures were observed (Figure 4, E). These early stage capsid complexes subsequently assemble into circular intermediates (Figure 4, F and G), followed by formation of icosahedral capsids with a small opening on one side (Figure 4, H) and progressive recruitment of electron dense materials. Nucleocapsids were observed in a partially filled state (Figure 4, I) as well as fully filled (Figure 4, J).

Peer-reviewed version available at *Viruses* **2019**, *11*, 354; doi:10.3390/v11040354

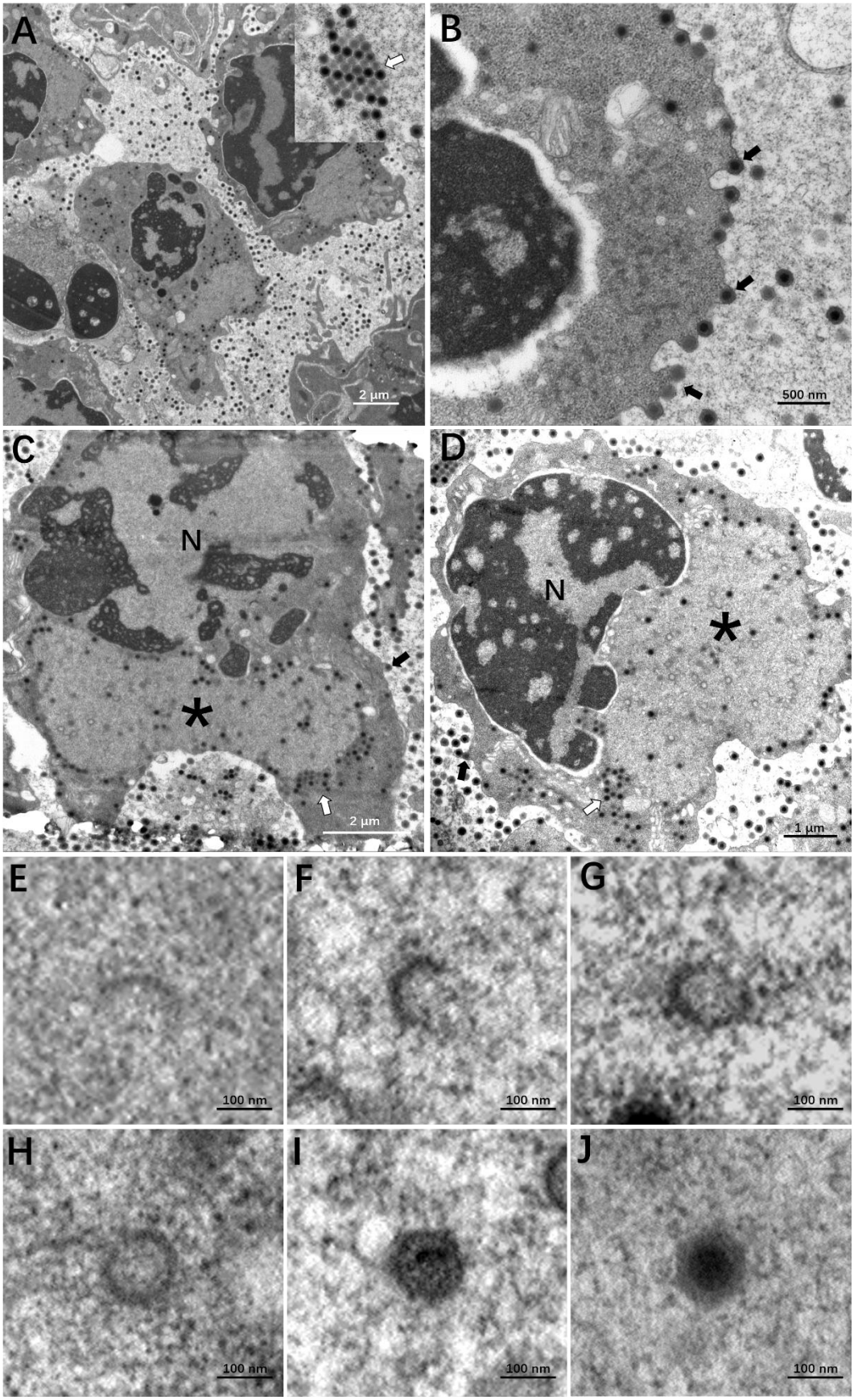

Figure 4. TEM of hematopoietic tissue of naturally infected *M. rosenbergii* samples 20180620. **A**: A large numbers of virions in hematopoietic tissue; **B**: SHIV budded from the plasma membrane; **C** and **D**: SHIV replication and assembly in hematopoietic cell; **E:** Crescent-shaped structures; **F-I:** As the packing process continues, the crescent-shaped structure curves to form icosahedral capsids; **J:**

Mature virions with a dense core are eventually formed. N: nucleus; *: a large electron-lucent virogenic stroma; black arrows: budding virions; and white arrows: paracrystalline array of virus particles.

3.6 Quantitative detection of SHIV in different tissues of natural infected M. rosenbergii

Total 120 tissues were separated from 15 natural infected prawns *M. rosenbergii*. SHIV loads in tissues of different prawns were examined by TaqMan qPCR. The copies of SHIV per μg tissue DNA sample were converted to their logarithms for calculation of the geometric means and standard deviations of each tissue. The results showed that hematopoietic tissue samples contained an average SHIV load at $10^{(7.92\pm0.91)}$ copies/μg-DNA, which was the highest load of SHIV in tissues tested. Antenna had a mean SHIV load at $10^{(7.84\pm0.70)}$ copies/μg-DNA, which was approached to hematopoietic tissue. Uropods, pleopods, gills and pereiopods had also high loads of SHIV above $10^{7.6}$ copies/μg-DNA of geometric means. Moreover, muscle and hepatopancreas, as the vast majorities of cephalothorax and abdominal segments of the prawn, contained the lowest load of SHIV, which was at $10^{(6.96\pm0.57)}$ and $10^{(6.85\pm0.72)}$ copies/μg-DNA, respectively (Table 2). It was also noticed that there were big differences of SHIV loads by 3—4 orders of magnitude in all of the tissues among different individuals showed in the range column of Table 2.

Table 2. SHIV copies in different tissues detected in SHIV-positive prawns *Macrobrachium rosenbergii*.

Samples	n	Geometric mean (copies/μg-DNA)	Range (copies/μg-DNA)
Hematopoietic tissue	15	$10^{(7.92\pm0.91)}$	8.11×10^{4} — 6.33×10^{8}
Antenna	15	$10^{(7.84\pm0.70)}$	1.44×10^{6} — 1.03×10^{9}
Uropods	15	$10^{(7.74\pm0.71)}$	6.45×10^{5} — 6.04×10^{8}
Pleopods	15	$10^{(7.77\pm0.69)}$	4.77×10^{5} — 5.30×10^{8}
Gills	15	$10^{(7.69\pm0.66)}$	4.45×10^{5} — 4.10×10^{8}
Pereiopod	15	$10^{(7.62\pm0.69)}$	6.10×10^{5} — 1.05×10^{9}
Muscle	15	$10^{(6.96\pm0.57)}$	1.87×10^{5} — 4.36×10^{7}
Hepatopancreas	15	$10^{(6.85\pm0.72)}$	2.35×10^{4} — 3.18×10^{7}

3.7 Relative abundance of SHIV in different tissues

As the differences of SHIV loads in tissues among different individuals reached 3—4 orders of magnitude, the direct comparison on SHIV loads in a specific tissue could be easily upset by a single sample with a very high SHIV load. Therefore, relative abundance of SHIV load based on a uniformization of the sum of SHIV loads in all detected tissues was introduced to evaluate the distribution of SHIV in different tissues. The relative abundance results showed that more than 1/4 of SHIV relative load in hematopoietic tissue, which contained the highest relative abundance at (25.4±16.9)%. Antenna, pleopods, and uropods contained significantly lower SHIV relative abundance at (18.7±10.3)%, (14.5±5.1)%, and (13.8±4.7)%, respectively, than hematopoietic tissue did (P<0.05). Gills and pereiopods contained the very significant lower SHIV relative abundance at (12.1±4.1)% to (10.7±5.5)%, respectively, than hematopoietic tissue did (P<0.01). Hepatopancreas and muscle contained the very significantly lowest levels of the relative abundances of SHIV at (2.44±2.16)% (2.44±1.24)% and comparing with all other tissues (P<0.01), respectively (Figure 5). When the total SHIV load in all tissues fell between $10^{8.24}$ to $10^{9.25}$ copies/μg-DNA, most of the relative abundances of SHIV in hematopoietic tissue fell into 12.2% to 35.9%, even 71.7%; however, when the total SHIV load in all tissues was lower than 10^{7} or higher than $10^{9.5}$ copies/μg-DNA, the relative abundances of SHIV dropped to about 5% or lower level.

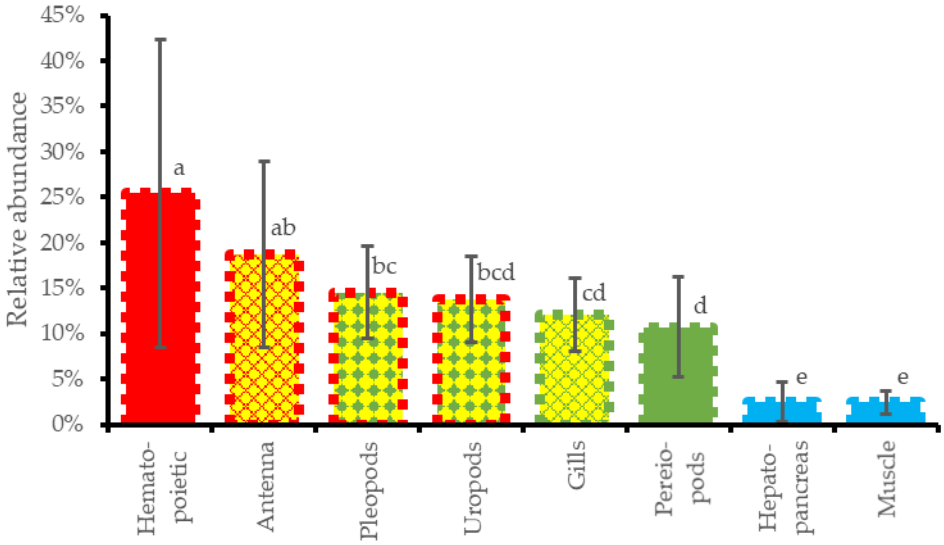

Figure 5. Relative abundance of SHIV for different tissues of fifteen SHIV-infected *M. rosenbergii* samples. No same letter sharing on the columns indicates significant difference ($P<0.05$); no same color sharing in the columns indicates highly significant difference ($P<0.01$).

4. Discussion

SHIV was found in farmed *P. vannamei* collected in a shrimp pond suffering from unknown disease in Zhejiang Province in Dec. 2014. Phylogenetic analysis revealed that the virus should belong to a new genus, temporarily named as *Xiairidovirus*, under family *Iridoviridae* [1, 2]. Latterly, alignment of genome sequences revealed the virus shares 99% identical with the previously reported virus CQIV found in red claw crayfish *C. quadricarinatus* collected from a market in Fujian Province in June 2014 [4, 5]. Recently, the iridovirus group of ICTV discussed these two reports and proposed a new genus name *Decapodiridovirus*. Target surveillance has been started in China in 2017 and revealed that the virus has been detected in 6 provinces out of 13 surveyed provinces and caused massive economic losses [14].

As far as we know, there were no pathological information of *M. rosenbergii* infected with SHIV available, but a PCR detection result showed that 5 of 33 cultured *M. rosenbergii* samples were SHIV positive from 2014 to 2016 [1]. This study reported farmed *M. rosenbergii* and *Pr. clarkii* and cohabitating with some wild crustacean, *M. nipponense*, *M. superbum* and Cladocera in a pond in Jiangsu Province suffered from severe mortality in June 2018, following the *P. vannamei* population dying out in the adjacent pond. The diseased giant freshwater prawns exhibited a typical symptom commonly known as 'white head' or 'white spot' since 2015 [15]. Real-time PCR results showed that all samples were negative for WSSV, IHHNV, *Vp*$_{AHPND}$, YHV, IMNV and CMNV, but positive for SHIV. Samples of *M. rosenbergii* contained the highest SHIV loads range from 3.16×10^8 to 9.83×10^8 copies/μg-DNA, which were higher than any other natural infected species in this study and earlier report [3], indicated that the disease of *M. rosenbergii* in this case was caused by a severe infection with SHIV. This is the first confirmation for the causative agent of 'white head' symptom in farmed *M. rosenbergii*. And in this case, SHIV was also proved to be a natural pathogen to *P. clarkii* and *M. nipponense*. The disease firstly outbroke and caused dying out in farmed *P. vannamei* population in the adjacent pond two weeks before clinical signs of prawns were found in the pond stocking *M. rosenbergii*. It provided an evidence that the disease transmitted cross ponds and species due to lack of biosecurity in the farm management.

Notably, the susceptibilities of *M. rosenbergii*, *M. nipponense*, *P. vannamei*, and *Pr. clarkii* to infection with SHIV and infection with WSSV are different. Earlier study revealed that *M. rosenbergii* and *M. nipponense* resisted to infection with WSSV via intermuscular injection, while *Pr. clarkii* was infected with high mortality of 94% [21]. Further challenge studies showed *M. rosenbergii* could be infected by injection with WSSV stains Thai-1 and Viet, however, the infectious dose to

reach 50% endpoint in *M. rosenbergii* needed 20-fold and 400-fold more than that in *P. vannamei*, respectively [22]. The half lethal dose (LD50) of WSSV to *M. nipponense* by injection was $10^{(3.84\pm0.06)}$ copies/g, which was about 1780-fold higher than that to *P. vannamei* at $10^{(0.59\pm0.22)}$ copies/g [23]. It was demonstrated that *M. rosenbergii* could clear injected infectious WSSV after 5 to 50 days post-injection [24]. There is no report for the quantitative comparison on the virulence of SHIV to different species yet. Based on the time course of mortality in intramuscular challenge with SHIV, *P. vannamei* may be a little bit more susceptible to SHIV infection than *C. quadricarinatus* and *Pr. clarkii* [4]. The disease course observed in the farm of this study indicated that *M. rosenbergii* and *M. nipponense* has no tolerance to the infection with SHIV. Many farms in Jiangsu, Guangdong, and Zhejiang Provinces [25, 16], as well as in Southeast Asia [26, 27] and Africa [28] have stocked ponds in polyculture mode with *M. rosenbergii* and *P. vannamei* or *P. monodon*. As *M. rosenbergii* has tolerance to infection with WSSV [21], the polyculture mode provides a profitable approach for farmers under the threat of WSSV. However, emerging of SHIV has shattered that vision and verified our earlier warning that polyculture with different species of crustacean may bring risks for spread of disease, increase of susceptible species, and evolution of pathogens, based on our early surveillance on shrimp epidemiology [29].

M. rosenbergii and *P. vannamei* infected with SHIV both exhibited hepatopancreatic atrophy with colour fading on the surface and in the section, empty stomach and guts. However, these symptoms are not distinctive, because empty stomach and guts also occurred in some other diseases, such as infection with WSSV [17,30], infection with Taura syndrome virus (TSV) and AHPND [17], and loss color of hepatopancreas is similar to the clinical feature of AHPND [17]. It's worth noting that 'white head' is a typical clinical sign for on-site diagnosis to *M. rosenbergii* infected with SHIV. Xu et al [4] reported that experimental challenged individuals of *Pr. clarkii* showed gross signs such as cessation of feeding and flaccidity at day 5 post-infection. In this case, cultured *Pr. clarkii* natural infected with SHIV contained a lower viral load (2.20×10^3 to 1.57×10^4 copies/μg-DNA) and suffered from an asymptomatic infection, because it was just at day 3 after the juveniles of crayfish were stocked in the pond. Almost all of shrimp *P. vannamei* in the adjacent pond died out in two weeks and were abandoned by drainage. It was one month later when we arrived in the farm, and only several dried bodies of *P. vannamei* could be collected from the bottom of drained pond which could not be used for observation of gross signs.

Histopathological examination showed the existence of dark eosinophilic inclusions mixed or surrounded with basophilic staining and karyopyknosis in the hematopoietic tissues and hemocytes of gills and hepatopancreatic sinus in *M. rosenbergii*. Similar pathological feature also existed in *M. nipponense* collected in this study and *Exopalaemon carinicauda* experimentally challenged with SHIV [20]. The inclusions of SHIV infection found in *P. vannamei* in previous research were described as basophilic, but the color of the inclusions on the published pictures was dark eosinophilic mixed with tiny basophilic staining as same as this study [1]. The eosinophilic inclusions were present in the cytoplasmic area in hemocytes or hematopoietic cells, which is very similar to some shrimp cases caused by the iridescent virus earlier reported [31, 32], and the karyopyknosis is similar to some fish cases [33, 34]. Similar as ISH, ISDL also specifically indicated the existence and location of SHIV in histologic sections. Blue signals were observed in hematopoietic tissue and hemocytes in sinus of hepatopancreas and gills in *M. rosenbergii*, *M. nipponense*, and *Pr. clarkii*, which is consistent with the ISH results in sections of infected *P. vannamei* [1]. However, differing from the results of ISH, positive signals resulted from ISDL were also observed in some R-cells and myoepithelial fibers of hepatopancreas, coelomosac epithelium of antennal gland, and epithelium of ovaries, which indicated that besides hematopoietic tissues and hemocytes, SHIV may also infect some other tissues. And, more remarkable, blue signals of ISDL appeared in both nucleus and cytoplasm of hematopoietic cells, hemocytes and other infected cells. It signified that SHIV may employ a replication strategy to include both nuclear and cytoplasmic stages, as Frog virus 3 (FV3), the typical species of genus *Ranavirus*, does [35-37]. Compared with the ISH in *P. vannamei* [1], it should be borne in mind that the amplification of target DNA in ISDL results in a similar climax quantity of amplified products, so that the density of positive signals does

not relatively reflect the original quantity of DNA target, and can only indicated the presence and location of target viral nucleic acid in the cells of various tissues and organs [38].

TEM evidences also proved the diseased prawns *M. rosenbergii* were infected with SHIV by viral morphology and cytopathology. The icosahedral morphology and intracytoplasmic location of virions are consistent with reports of SHIV infections in *P. vannamei* [1] or CQIV in *C. quadricarinatus*, *Pr. clarkii* and *P. vannamei* [4]. Non-enveloped virions were (166.3±14.8) nm (v-v) and (149.4±13.8) nm (f-f), with a nucleoid at (93.5 ± 9.9) nm, which were 7.7 nm, 5.8 nm and 7.7 nm larger than previous study in *P. vannamei* [1]. The different size of virions may be resulted from different shrinkage of virions caused by the duration time of tissue samples stored in the TEM fixative and the dehydration and embedding procedures before ultrathin sectioning. Typical electron-lucent virogenic stroma was observed in hematopoietic cells of infected *M. rosenbergii*, containing immature, empty and mature virions, with paracrystalline array of virus particles and budding virions in the same cell. The appearance and location of virogenic stroma was consistent with the dark eosinophilic inclusions observed on the H&E stained histopathological slides, while viral nucleic acid, intensive mature virions, and paracrystalline array within and surrounding of the virogenic stroma resulted in the dark eosinophilic and tiny basophilic staining. The progressive curvature change from crescent shape to hexagonal capsid is very similar to the forming process of Singapore grouper iridovirus (SGIV) capsid [39], which was not reported for SHIV or CQIV in previous study.

TaqMan qPCR specifically detected the highest loads of SHIV in the whitish focal lesion of hematopoietic tissue under the carapace at the base of rostrum of diseased *M. rosenbergii*. This data filled the gap in the previous study on the SHIV load in the hematopoietic tissue [3]. Unlike *M. rosenbergii*, *P. vannamei* has several very small hematopoietic tissues, which make it hard to be seen and collected for quantitative detection of SHIV. Decapods have separate hematopoietic tissues locating above the stomach and at the base of antennas, pereiopods, and gills as appendages of the cephalothorax [19]. That's why the appendages under the cephalothorax also contained relative higher SHIV load than the main body. It's notable that the high loads of SHIV also detected in the appendages of the abdominal segments, including uropods and pleopods, which hinted that these appendages of abdominal segments may be attached with some hematopoietic cells. Muscle and hepatopancreas contained the lowest SHIV loads which may due to the virus in hemocytes and hemolymph in these tissues. The relative abundances of SHIV load in different tissues calculated based on the results of TaqMan qPCR could be used to quantitatively estimate the virus distribution for tissue tropism study in comparison with different hosts. Interestingly, the naturally dried bodies of shrimp *P. vannamei* died for more than one month could still be detected positive up to 7.19×10^6 copies/μg-DNA. It indicated that dried shrimp bodies are still available for SHIV detection but the infectivity of SHIV in the dried shrimp bodies needs to be further investigation.

5. Conclusions

This is the first report of a naturally occurrence of SHIV in farmed giant freshwater prawn *M. rosenbergii*. All of the evidences resulted from symptom description, detection of known pathogens, histopathological and cytopathological observation, *in situ* DIG-labeled LAMP location, and quantitative detection of tissues consistently confirmed that 'white head' symptom of *M. rosenbergii* is the typical signs caused by infection with SHIV. Additionally, this study also provided evidences to add *Pr. clarkii* and *M. nipponense* as the susceptible species of SHIV. The disease was likely transmitted from the adjacent pond stocked with *P. vannamei* which had died out during the outbreak of infection with SHIV due to lock of biosecurity in the farm management. The study provides a typical example how SHIV threaten the freshwater polyculture modes with different species of crustacean which we earlier discouraged.

Author Contributions: Conceptualization, L.Q., J.H. and Q.L.Z.; Formal analysis, L.Q. and X.C.; Funding acquisition, J.H.; Sampling, L.Q., X.C. , J.H. and R.H.Z.; Methodology, X.C., R.H.Z., C.L. and W.G.; Sample testing, X.C., R.H.Z., and W.G.; Project administration, J.H. and L.Q.; Resources, L.Q., X.C. and R.H.Z.; Supervision, J.H.; Writing—original draft, L.Q; Revision, J.H and L.Q.

Funding: This research was financially supported by Projects Under the Pilot National Laboratory for Marine Science and Technology (Qingdao) (QNLM201706), the Marine S&T Fund of Shandong Province for Pilot National Laboratory for Marine Science and Technology (Qingdao) (2018SDKJ0502-3), China ASEAN Maritime Cooperation Fund Project (2016–2018), and China Agriculture Research System, grant number CARS-48.

Acknowledgments: We are grateful to Prof. Guo-Liang Yang of Jiangsu Shufeng Aquatic Seed Industry Co. Ltd. for connecting the diseased farm, the agent serving the farm and the farmers in Jiangsu Province for their help during our sampling, as well as all of our laboratory members for their technical advice and helpful discussions.

Conflicts of Interest: The authors declare no conflict of interest. The funders had no role in the design of the study; in the collection, analyses, or interpretation of data; in the writing of the manuscript, and in the decision to publish the results.

References

1. Qiu, L.; Chen, M.M.; Wan, X.Y.; Li, C.; Zhang, Q.L.; Wang, R.Y.; Cheng, D.Y.; Dong, X.; Yang, B.; Wang, X.H.; Xiang, J.H.; Huang, J. Characterization of a new member of Iridoviridae, Shrimp hemocyte iridescent virus (SHIV), found in white leg shrimp (*Litopenaeus vannamei*). *Sci. Rep.* **2017**, *19*, 11834, doi: 10.1038/s41598-017-10738-8.
2. Qiu, L.; Chen, M.M.; Wang, R.Y.; Wan, X.Y.; Li, C.; Zhang, Q.L.; Dong, X.; Yang, B.; Xiang, J.H.; Huang, J. Complete genome sequence of shrimp hemocyte iridescent virus (SHIV) isolated from white leg shrimp, *Litopenaeus vannamei*. *Arch. Virol.* **2018**, *163*, 781-785, doi: 10.1007/s00705-017-3642-4.
3. Qiu, L.; Chen, M.M.; Wan, X.Y.; Zhang, Q.L.; Li, C.; Dong, X.; Yang, B.; Huang, J. Detection and quantification of shrimp hemocyte iridescent virus by TaqMan probe based real-time PCR. *J. Invertebr. Pathol.* **2018**, *154*, 95-101, doi: 10.1016/j.jip.2018.04.005.
4. Xu, L.; Wang, T.; Li, F.; Yang, F. Isolation and preliminary characterization of a new pathogenic iridovirus from redclaw crayfish *Cherax quadricarinatus*. *Dis. Aquat. Organ.* **2016**, *120*, 17-26, doi: 10.3354/dao03007
5. Li, F.; Xu, L.; Yang, F. Genomic characterization of a novel iridovirus from redclaw crayfish *Cherax quadricarinatus*: evidence for a new genus within the family *Iridoviridae*. *J. Gen. Virol.* **2017**, *98*, 2589-2595, doi: 10.1099/jgv.0.000904.
6. Ramsden N. and Smith J. Clarification. Shrimp disease SHIV detected in China, Thailand, but not Vietnam. undercurrentnews, 2018-10-1. https://www.undercurrentnews.com/2018/10/01/clarification-shrimp-disease-shiv-detected-in-china-thail and-but-not-vietnam/
7. Rao, R.; Bhassu, S.; Bing, R.Z.; Alinejad, T.; Hassan, S.S.; Wang, J. A transcriptome study on *Macrobrachium rosenbergii* hepatopancreas experimentally challenged with white spot syndrome virus (WSSV). *J. Invertebr. Pathol.* **2016**, *136*, 10-22, doi: 10.1016/j.jip.2016.01.002.
8. Hameed, A.S.S. Viral infections of *Macrobrachium* spp.: Global status of outbreaks, diagnosis, surveillance, and research. *Israeli Journal of Aquaculture-Bamidgeh* **2009**, *61*, 240-247,
9. Ho, K.L.; Gabrielsen, M.; Beh, P.L.; Kueh, C.L.; Thong, Q.X.; Streetley, J.; Tan, W.S.; Bhella, D. Structure of the *Macrobrachium rosenbergii* nodavirus: a new genus within the Nodaviridae? *PLoS Biol.* **2018**, *16*, e3000038, doi: 10.1371/journal.pbio.3000038.
10. FAO. *Macrobrachium rosenbergii* (De Man, 1879): Fishers and Aquaculture Department, Food and Agricultural Organization of the United Nations; 2017 [cited 2018 August 3]. Available from: http://www.fao.org/fishery/culturedspecies/Macrobrachium_rosenbergii/en.
11. Bonami, J.R.; Sri Widada J. Viral diseases of the giant fresh water prawn *Macrobrachium rosenbergii*: a review. *J. Invertebr. Pathol.* **2011**, *106*, 131-42, doi: 10.1016/j.jip.2010.09.007.
12. Sahul Hameed, A.S.; Bonami, J.R. White tail disease of freshwater prawn, *Macrobrachium rosenbergii*. *Indian J. Virol.* **2012**, *23*, 134-40, doi: 10.1007/s13337-012-0087-y.
13. Zhang, Q.L.; Xu, T.T.; Wan, X.Y.; Liu, S.; Wang, X.H.; Li, X.P.; Dong, X.; Yang, B.; Huang, J. Prevalence and distribution of Covert mortality nodavirus (CMNV) in cultured crustacean. *Virus. Res.* **2017**, *233*, 113-119, doi: 10.1016/j.virusres.2017.03.013.
14. Qiu, L.; Dong, X.; Wan, X.Y.; Huang, J. Analysis of iridescent viral disease of shrimp (SHID) in 2017. In *Analysis of Important Diseases of Aquatic Animals in China in 2017* (in Chinese). Fishery and Fishery Administration Bureau under the Ministry of Agriculture and Rural Affairs, National Fishery Technical Extension Center, Eds.; China Agriculture Press, Beijing, 2018; pp. 187-204, ISBN 978-7-109-24522-8.
15. Qi, R.R.; Cui, L.B.; Zhang, H.J.; Tang, Z.L.; Zhang, W.W.; Tan, X.Y. Who is the ringleader of the "white spot" disease in *Macrobrachium rosenbergii*. Chinese Aquaculture Web, 17 May, **2016**, http://www.shuichan.cc/article_view-41757.html (in Chinese), accessed on 9 Jan. 2019.
16. Huang, S. Polyculture of *Macrobrachium rosenbergii* and *Litopenaeus vannamei* will become the main mixed culture mode in Chaozhou and Shantou of Guangdong Province. *Chinese Aquaculture Gateway Web*, **2015**, http://www.bbwfish.com/article.asp?artid=173520 (in Chinese), accessed on 9 Jan. 2019.
17. OIE. Aquatic Animal Health Code. Paris: World Organization for Animal Health. (2017).
18. Zhang, Q.L.; Liu, Q.; Liu, S.; Yang, H.L.; Liu, S.; Zhu, L.L.; Yang, B.; Jin, J.T.; Ding, L.X.; Wang, X.H.; Liang, Y.; Wang, Q.T.; Huang, J. A new nodavirus is associated with covert mortality disease of shrimp. *J. Gen. Virol.* **2014**, *95*, 2700-9, doi: 10.1099/vir.0.070078-0.
19. Bell, T. A. & Lightner, D. V. A Handbook of Normal Penaeid Shrimp Histology. Baton Rouge, LA: World Aquaculture Society (1988).

20. Chen, X.; Qiu, L.; Wang, H.L.; Zou, P.Z.; Dong, X.; Li, F.H.; Huang, J. Susceptibility of *Exopalaemon carinicauda* to the infection with Shrimp hemocyte iridescent virus. *Virus* (under review).
21. Huang, C.H.; Shi, Z.L.; Zhang, J.H.; Zhang, L.R.; Chen D.H.; Bonami, J.R. Establishment of a model for proliferating White spot syndrome virus in vivo. *Virologica Sinica* **1999**, 14(4), 358-363.
22. Corteel, M.; Dantas-Lima, J.J.; Tuan, V.V.; Thuong, K.V.; Wille, M.; Alday-Sanz, V.; Pensaert M.B.; Sorgeloos, P.; Nauwynck, H.J. Susceptibility of juvenile *Macrobrachium rosenbergii* to different doses of high and low virulence strains of white spot syndrome virus (WSSV). *Dis. Aquat. Org.* **2012**, 100, 211–218, doi: 10.3354/dao02496.
23. Zhao, C.Y.; Fu, H.T.; Sun, S.M.; Qiao, H.; Zhang, W.Y.; Jin, S.B.; Jiang, S.F.; Xiong, Y.W.; Gong, Y.S. Experimental inoculation of oriental river prawn *Macrobrachium nipponense* with white spot syndrome virus (WSSV). *Dis. Aquat. Org.* **2017**, 126, 125–134, doi: 10.3354/dao03165.
24. Sarathi, M.; Nazeer Basha, A.; Ravi, M.; Venkatesan, C.; Senthil Kumar, B.; Sahul Hameed, A.S. Clearance of white spot syndrome virus (WSSV) and immunological changes in experimentally WSSV-injected *Macrobrachium rosenbergii*. Fish & Shellfish Immunol. **2008**, 25(3), 222-230, doi: 10.1016/j.fsi.2008.04.011.36. Chinchar, V.G.; Hyatt, A.; Miyazaki, T.; Williams, T. Family *Iridoviridae*: poor viral relations no longer. *Curr. Top. Microbiol. Immunol.* **2009**, *328*, 123-70.
25. Shen, Y.J.; Zhu, B.K.; Xu, K.C.; Xu, J.F. Pond culture experiment of polyculture with white leg shrimp and *Macrobrachium rosenbergii*. *Modern Agricultural Technology* (in Chinese), **2017**, 17, 231 & 241.
26. Azim, M.E.; Mazid, M.A.; Alam, M.J.; Nurullah, M. The potential of mixed culture of freshwater giant prawn *Macrobrachium rosenbergii* de Man and tiger shrimp *Penaeus monodon* Fab. at Khulna region, Bangladesh. *Bangladesh J. Fish. Res.* **2001**, 5(l), 67-74, http://120.52.51.17/aquaticcommons.org/17691/1/BJFR5.1_067.pdf.
27. Ali, H.; Rahman, M.M.; Rico, A.; Jaman, A.; Basak, S.K.; Islam, M.M.; Khan, N.; Keus, H.J.; Mohan, C.V. An assessment of health management practices and occupational health hazards in tiger shrimp (*Penaeus monodon*) and freshwater prawn (*Macrobrachium rosenbergii*) aquaculture in Bangladesh. *Vet. Ani. Sci.* **2018**, 5, 10-19, doi: 10.1016/j.vas.2018.01.002.
28. Sadek, S.; Moreau, J. Performance of *Macrobrachium rosenbergii* and *Penaeus semisulcatus* under mono and mixed culture systems, and their suitability for polyculture with Florida Red Tilapia, in Egypt. *J. Aquaculture in the Tropics* **2000**, 15(2), 97-107.
29. Huang J. Diseases of farmed shrimp and their biosecurity control technologies (2015-12-22). *Chinese Aquaculture Web*, **2015**, http://www.shuichan.cc/news_view-268040.html (in Chinese), accessed on 9 Feb. 2019.
30. Escobedo-Bonilla, C.M.; Alday-Sanz, V.; Wille, M.; Sorgeloos, P.; Pensaert, M.B.; Nauwynck, H.J. A review on the morphology, molecular characterization, morphogenesis and pathogenesis of White spot syndrome virus. *J. Fish. Dis.* **2008**, *31*, 1-18, doi: 10.1111/j.1365-2761.2007.00877.x.
31. Lightner, D. V. & Redman, R. M. A putative iridovirus from the penaeid shrimp *Protrachypene precipua* Burkenroad (Crustacea: Decapoda). *J. Invertebr. Pathol.* 62, 107–109 (1993).
32. Tang, K. F. J. et al. Identification of an iridovirus in *Acetes erythraeus*, (Sergestidae) and the development of *in situ*, hybridization and PCR method for its detection. *J. Invertebr. Pathol.* 96, 255–260 (2007).
33. Mahardika, K., Yamamoto, A. & Miyazaki, T. Susceptibility of juvenile humpback grouper *Cromileptes altivelis* to grouper sleepy disease iridovirus (GSDIV). *Dis. Aquat. Org*. 59, 1–9 (2004).
34. Sudthongkong, C.; Miyata, M.; Miyazaki, T. Iridovirus disease in two ornamental tropical freshwater fishes: African lampeye and dwarf gourami. *Dis. Aquat. Org*. **2002**, 48, 163–173.
35. ICTV Reports: *Iridoviridae*. Available online: https://talk.ictvonline.org/ictv-reports/ictv_online_report/dsdna-viruses/w/iridoviridae
36. Chinchar, V.G.; Hyatt, A.; Miyazaki, T.; Williams, T. Family *Iridoviridae*: poor viral relations no longer. *Curr. Top. Microbiol. Immunol.* **2009**, *328*, 123-70.
37. Williams, T.; Barbosa-Solomieu, V.; Chinchar, V.G. A decade of advances in iridovirus research. *Adv. Virus Res.* **2005,** *65*, 173-248, doi: 10.1016/S0065-3527(05)65006-3.
38. Jitrakorn, S.; Arunrut, N.; Sanguanrut, P.; Flegel, T.W.; Kiatpathomchai, W.; Saksmerprome, V. *In situ* DIG-labeling, loop-mediated DNA amplification (ISDL) for highly sensitive detection of infectious hypodermal and hematopoietic necrosis virus (IHHNV). *Aquaculture* **2016**, *456*, 36-43, doi: 10.1016/j.aquaculture.2016.01.023.

39. Liu, Y.; Tran, B.N.; Wang, F.; Ounjai, P.; Wu, J.; Hew, C.L. Visualization of assembly intermediates and budding vacuoles of Singapore grouper iridovirus in grouper embryonic cells. *Sci. Rep.* **2016**, 6, 18696, doi: 10.1038/srep18696.